Physics and Chemistry of Minerals (2025) 52:30
https://doi.org/10.1007/s00269-025-01331-x

REVIEW ARTICLE

Revisiting claims of natural monocrystalline lonsdaleite: a re-assessment of published data

Thomas E. Weirich[1]

Received: 18 June 2025 / Accepted: 13 September 2025

Abstract
This study re-evaluates the selected area electron diffraction (SAED) patterns and electron energy-loss spectrum (EELS) presented by Shumilova et al. (https://doi.org/10.1134/S1028334X11110201), who have reported that they have found natural hexagonal 2H diamond in samples from the Kumdykol (Kumdy-Kol) diamond deposit. A thorough re-evaluation of the original SAED data indicates that a diffraction pattern previously attributed to monocrystalline 2H diamond is, with a very high degree of certainty, not the claimed phase, since it exhibits a much stronger resemblance with the calculated pattern of a high-pressure phase of 2H graphite, and even more with the pattern of a cubic, high-pressure form of silicon carbide. Due to the absence of EDX data, the question regarding the precise composition of this crystalline species could not be conclusively resolved. Furthermore, a second SAED pattern, previously interpreted as a 3C–2H diamond intergrowth, was found compatible with a topotactic 2H graphite–3C mineral association, known as 'diaphite', or with sp^3-bonded polytypes (3C–2*n*H, $n=2$, 4). A carbon core-loss EEL spectrum, which was used in Shumilova et al. (Dokl Earth Sci 441:1552–1554, 2011) to confirm the presence of 2H diamond, was found to match with that of the 3C diamond structure. While these results do not rule out the natural occurrence of 2H diamonds in general, the re-assessment of the in Shumilova et al. (Dokl Earth Sci 441:1552–1554, 2011) published SAED and EELS data provides no concrete evidence for the presence of monocrystalline 2H diamond in the earlier examined specimens from the Kumdykol site. A correction of the in Shumilova et al. (Dokl Earth Sci 441:1552–1554, 2011) made claims is therefore of significance, to avoid further bias in the ongoing discussion on the nature of the mineral lonsdaleite.

Keywords Kumdykol (Kumdy-Kol) diamond deposit · Lonsdaleite · Hexagonal diamond · 2H diamond · Cubic diamond · 3C diamond · Selected area electron diffraction (SAED) · Electron energy-loss spectroscopy (EELS)

Introduction

In a widely recognized study with the title "Natural Monocrystalline Lonsdaleite", Shumilova et al. (Shumilova et al. 2011) reported in 2011 the discovery of natural monocrystalline 2H diamond (in the original publication, the term 'lonsdaleite' was used as a synonym for the 2H diamond structure) in carbon-rich mineral samples from the Kumdykol (or Kumdy-Kol) diamond deposit, Akmola Region, Kazakhstan. Due to the significance of these findings, the study has been widely cited in support of the natural occurrence of micrometre-size single crystals of hexagonal diamond (Bean et al. 2025; Zhu et al. 2025; Chen et al. 2024; Németh et al. 2023; Thomas et al. 2023; Tomkins et al. 2022; Murri et al. 2019; Fan et al. 2018; Turneaure et al. 2017; Daulton et al. 2017; Jones et al. 2016; Boslough et al. 2012). However, aside the ongoing discussion within the scientific community regarding the natural occurrence of crystals with 2H diamond structure (see for example (Daulton et al. 2010; Greshnyakov and Belenkov 2017; Németh et al. 2014) and the review by Dobrzhinetskaya et al. (2022)), Németh et al. (2022) have recently raised questions about the validity of the in Shumilova et al. (2011) published results. As the main findings by Shumilova et al. (2011) are based on transmission electron microscopy (TEM) data collected at the authors' facility, the author of the present study considered it necessary to re-evaluate this data in order to resolve this

✉ Thomas E. Weirich
weirich@gfe.rwth-aachen.de

[1] Gemeinschaftslabor für Elektronenmikroskopie (GFE), RWTH Aachen University, Ahornstr. 55, 52074 Aachen, Germany

Published online: 10 October 2025

issue. The following is a comprehensive re-evaluation of the original SAED patterns and the published EEL spectrum.

Key-findings of the earlier report

In their article, Shumilova et al. (2011) report that 2H diamond was observed in the form of both individual monocrystalline crystals, with sizes of up to 5 µm, and extremely fine, platelet-shaped particles. According to the authors, 2H diamond was also found in coherent aggregates with cubic diamond (3C), forming superlattice-like structures, as well as in three-phase associations that included 2H graphite. In these composite structures, the (001) faces of 2H graphite are oriented perpendicular to the (111) planes of 3C diamond and the (001) faces of 2H diamond. To confirm the monocrystalline nature of 2H diamond, the authors used selected area electron diffraction (SAED) and electron energy-loss spectroscopy (EELS). The absence of a π* peak around 284 eV in the shown EEL spectrum was interpreted as evidence for purely sp^3-hybridised carbon and a prove for 2H diamond. Raman spectroscopy was also employed to assist identifying the phase in question. Since Raman analysis lies outside the scope of the present author's expertise, the following re-assessment will focus exclusively on the SAED and EELS data presented in Shumilova et al. (2011). However, in this particular context, the reader is referred to Németh et al. (2022), who found the Raman spectra presented by Shumilova et al. to be inconsistent with 2H diamond.

Re-assessment of the experimental SAED patterns

The original publication by Shumilova et al. (2011) includes two selected area electron diffraction (SAED) patterns, which are shown as smaller insets in the corresponding transmission electron microscopy (TEM) bright-field images. However, apart from some labels with diffraction spot indices on the SAED pattern, no additional information is provided, such as d-spacings or identified zone axis orientations. In order to avoid confusion with references to Figures in this article, in the following, the SAED patterns shown as insets in Figs. 1 and 4 in the original publications will be referred in the following as first and second SAED pattern. For the sake of transparency, both the original SAED patterns and the corresponding TEM bright-field images are shown here in full size for the first time in Fig. 1.

As documented by another TEM bright-field image (not shown here), the first SAED pattern in Fig. 1a was recorded at the position indicated by the white '×' in Fig. 1b. The TEM bright-field image shows an extended crystalline platelet with alternating bright and dark bands (commonly referred to as thickness or wedge fringes (McLaren 1991)) that reach from the rim of the particle up to the centre. The presence of these fringes up to the particles center indicates that the object must be very thin and made of a material with a low atomic number due to almost absent absorption. However, it should be noted that crystals with thickness fringes extending to the centre are very atypical in these samples, as well as in general. Based on the SAED pattern in Fig. 1a, the authors of Shumilova et al. (2011) attributed the pattern to a monophase, monocrystalline 2H diamond.

Figure 1c shows the second SAED pattern, which appears to originate from a more complex material. The corresponding TEM bright-field image (Fig. 1d) displays parallel 'lath-like' features of dark contrast. These lath-like features are regularly spaced and extend in three directions at 60-degree angles to each other. The dark 'lath-like' features overlap in some regions, have no sharp edges, and have a diameter of about 10 nm and a spacing of about the same size from each other. This arrangement has been interpreted in Shumilova et al. (2011) as a coherent superlattice-like structure, and the SAED pattern shown in Fig. 1c was attributed to a 3C diamond–2H diamond two-phase composite.

To avoid introducing own bias in the here described re-analysis of the SAED patterns by preselecting some structural data, it was mainly carried out with the program *SAED Extension* V1.3 included in the ICDD PDF-5+database (Kabekkodu 2024). The within this re-examination used camera constants for the employed FEI Tecnai F20 and Jeol 2000FX-II TEMs were recalculated from reference patterns of gold that were recorded at the time of the investigations. Refined lattice parameters from calibrated SAED patterns were obtained by help of the programs *UnitCellSAED* (Weirich 2025) and *UnitCell* (Holland and Redfern 1997).

Re-assessment for the SAED pattern of an ascribed monophase monocrystalline 2H diamond

The first pattern in question in Fig. 1a was analysed with the program *SAED Extension* to search the ICDD PDF database for identifying the most likely carbon phase and it´s corresponding zone axis orientation. A by *SAED Extension* provided quality parameter (FOM, figure of merit) for each hit, that values the agreement between the calculated and the user-defined experimental lattice, was employed to identify the most probable phases from the list of possible solutions. A list of 76 carbon-only structures was obtained for the pattern shown in Fig. 1a, with an allowed deviation of 5% in d-spacing and 3° in the angle of the user-defined 2D cell. Aside some unusual and unlikely carbon phases with primitive cubic, orthorhombic or trigonal lattices (which all do

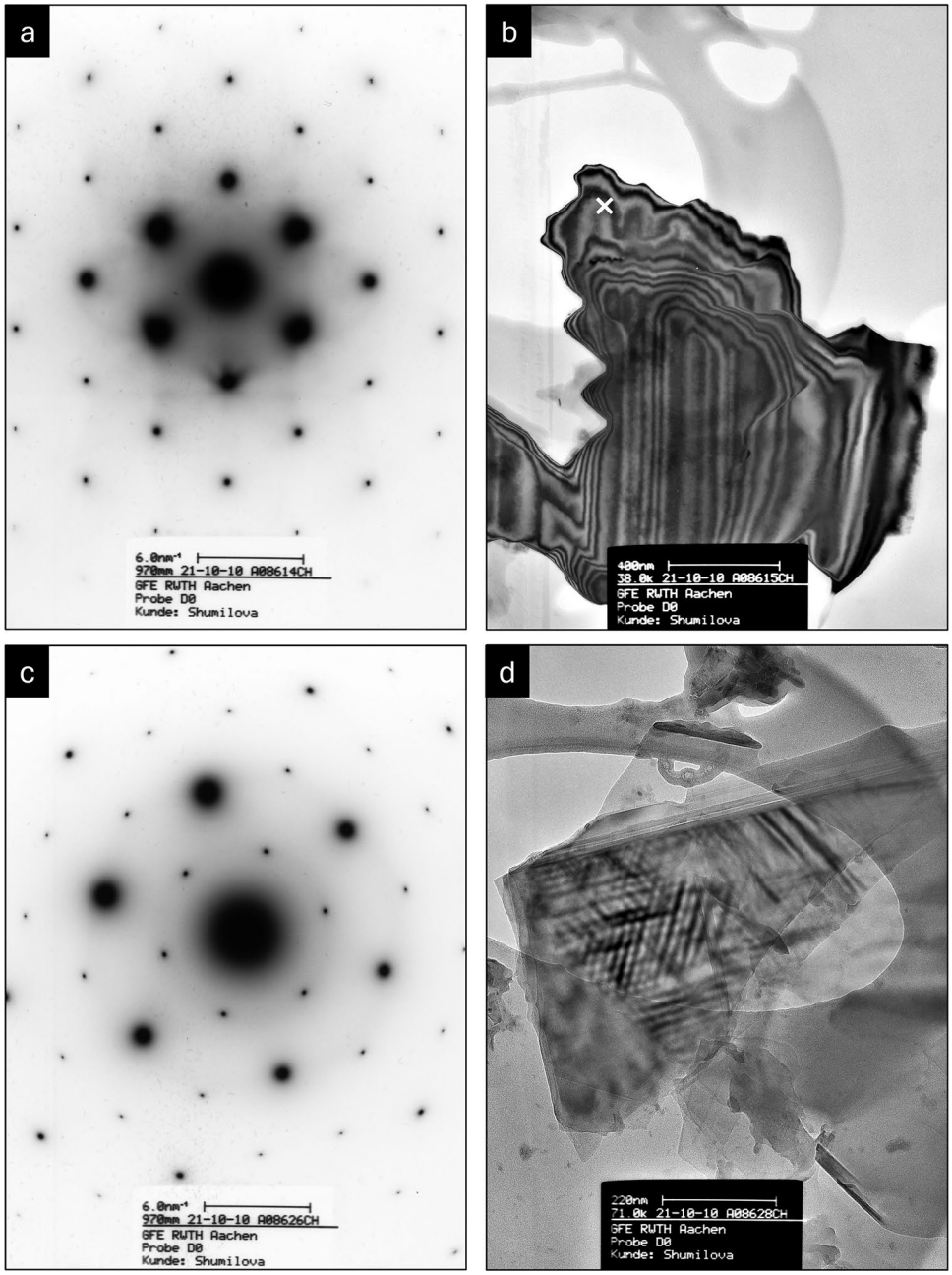

Fig. 1 Full-scale SAED patterns (inverted contrast) in **a**, **c** and TEM bright-field images in **b**, **d** that were used in the original article of Shumilova et al. (2011). The SAED pattern in **a** has been attributed by the authors to a monophase, monocrystalline 2H diamond crystallite and the pattern in **c** to a two-phase 3C–2H diamond composite (Image Source: GFE TEM Archive)

not match the whole geometry of the experimental SAED pattern) there were only 2H graphite (space group $P6_3/mmc$) and 3C diamond (space group $Fd\text{-}3\ m$) in the list, but no 2H diamond (space group $P6_3/mmc$). The latter is readily identified in the ranking list as the hexagonal 2H diamond phase has a lattice parameter c of approximately 4.1 Å, whereas the majority of the entries in the database for synthetic 2H graphite have a c-axis of around 6.7 Å. However, the most compatible match for the defined lattice with a FOM of 55 was found for zone axis [1 −1 −1] of a 2H graphite with lattice parameters $a = 2.5714$ Å, $c = 6.8382$ Å (PDF# 04-020-4354). The latter material is a product from high-pressure solid-state metathesis (HPSSM) synthesis at 1873 K and 5 GPa (Lei et al. 2013) and hence not unlikely as ultra-high-pressure metamorphic (UHPM) events have been associated with the recovering site (Dobrzhinetskaya et al. 2006). For the history and details on this research, the reader is referred to Dobrzhinetskaya et al. (2022). In striking contrast to this result, the best match for 3C diamond had a FOM value of 150 (PDF# 01-079-6061, $a = 3.577$ Å) for the [0 1 −1] orientation. Both suggested solutions are presented as overlays on the experimental SAED pattern in Figs. 2a, b. As Shumilova et al. did not specify a zone axis for the proposed 2H diamond phase in their report, the indices labels 101 and

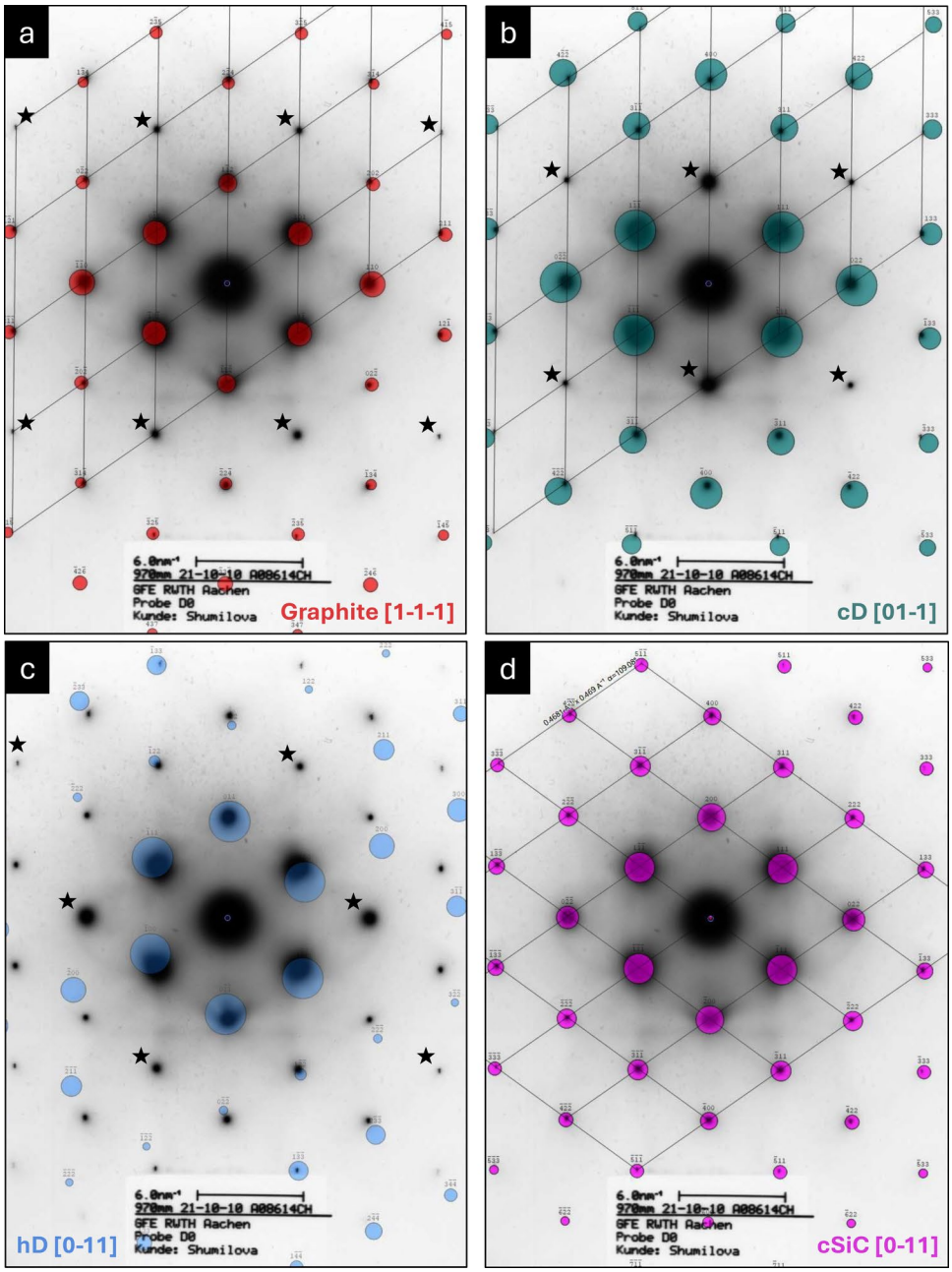

Fig. 2 Results from processing the SAED pattern from Fig. 1a with *SAED Extension* (ICDD PDF5+database, (Kabekkodu 2024)). As seen in **a**, the best match with the experimental pattern for carbon only phases were obtained for a HP 2H graphite (PDF# 04-020-4354, $P6_3/mmc$, $a=2.5714$ Å, $c=6.8382$ Å) with zone axis [1 −1 −1]. For comparison, Figure **b** shows the best match for 3C diamond (PDF# 01-079-6061, *Fd-3 m*, $a=3.577$ Å) with zone axis [0 1 −1]. The overlay for 2H diamond in **c** is the result of a trial-and-error search as the database search yielded no result for this phase due to the large deviations with experiment. The data for the latter were taken from PDF-file # 04-016-6276 ($P6_3/mmc$, $a=2.5239$ Å, $c=4.1213$ Å). As described in the main text, at a later stage SiC phases were also checked by a PDF5+database search. The one and only result of this search yielded a HP phase of cubic SiC (PDF-file # 04-006-7620, *Fm-3 m*, $a=3.684$ Å). The corresponding overlay for the found match is shown in **d**. As clearly visible, the match of the calculated pattern geometry for cubic SiC is very good and, with a FOM value of 4, about an order of magnitude better than found for the HP phase of 2H graphite in **a**. The refined lattice parameter for the F-cell in **d** is $a=3.696(4)$ Å. Kinematical forbidden diffraction spots, which commonly appear in SAED patterns, are marked with stars

100 provided by the earlier authors, were used to determine the corresponding zone axis. The therefrom calculated [010] zone axis orientation represents however, a rectangular reciprocal lattice cross-section, that is not compatible with the experimental SAED pattern. Since *SAED Extension* also failed to find a solution for 2H diamond, a trial-and-error search was carried out to find the zone axis with the closest geometric match. This approach led finally to the in Fig. 2c shown [0–11] orientation. The data used for simulation of the 2H diamond pattern were taken from PDF-file # 04-016-6276 ($P6_3$/mmc, $a=2.5239$ Å, $c=4.1213$ Å) since this was the best-found agreement for the in Sect. "Re-assessment for the SAED pattern from an ascribed two-phase 3C-2H diamond particle" carried out tests for the 2H diamond phase with the second SAED pattern (Fig. 1c). As indicated already by the very different FOM values and confirmed by visual comparison too, the solution found for 2H graphite in Fig. 2a is the most likely one as its best matches with the experimental pattern geometry among all items listed as pure carbon phases in the PDF5+database. In contrast, the simulated pattern for 2H diamond in Fig. 2c shows significant mismatches regarding spot positions and the 2D reciprocal cell angle. This is perhaps also the reason why *SAED Extension* has failed to find a solution for hexagonal diamond.

Based on this result, it must be concluded that the in Fig. 1b shown particle is with high probability 2H graphite and less likely cubic diamond, but definitely not 2H diamond, as claimed in Shumilova et al. (2011). This result is, however, based on the assumption that the investigated crystal is truly composed only of carbon. In order to exclude the possibility that the investigated crystal is a stressed and distorted 3C diamond, a lattice parameter refinement with the UnitCell program (Holland and Redfern 1997) was carried out for a cubic lattice. The latter yielded $a = 3.696 \pm 0.004$ Å from 26 d-spacings determined from the SAED pattern, which is significantly larger than for the approved 3C diamond in Fig. 3. Furthermore, the small standard deviation obtained for the refined lattice parameter is not consistent with a distorted cubic lattice. Though there exists a good agreement in the basic pattern geometry for <011> 3C diamond, the mismatch in lattice parameter is the reason for the poor FOM received with the SAED Extension program. To confirm that the SAED data had not been collected in error, the analysis was repeated using another pattern from a different thin crystal in the same sample that had the same appearance and morphology, as well as the same orientation. The refined lattice parameter found for this crystal was $a = 3.709 \pm 0.005$ Å, which confirmed the earlier obtained result. A subsequent search in the PDF5 + database for a material with this lattice parameter suggested (among other phases) cubic HP silicon carbide SiC (PDF-file # 04-006-7620, *Fm-3m*, $a = 3.684$ Å, (Yoshida et al. 1993)) as the most likely phase. This phase was considered as likely since SiC has earlier been approved to be present in related samples (Dobrzhinetskaya et al. 2022; Tretiakova and Lyukhin 2017). Processing of the pattern in Fig. 1a with SAED Extension, and focusing strictly

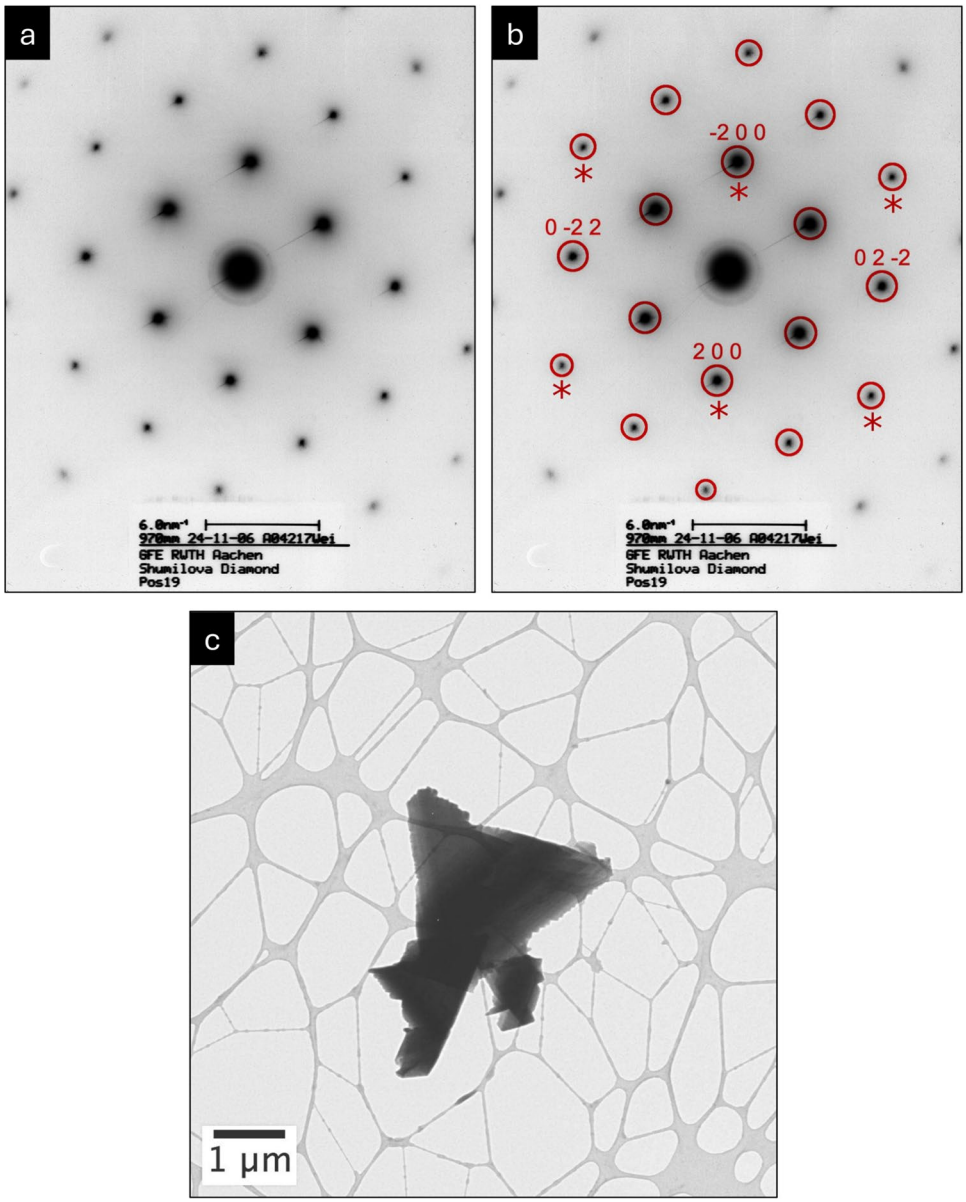

Fig. 3 SAED <011> pattern in **a** and corresponding TEM bright-field image in **c** from a verified cubic microdiamond that was investigated by the present author during a 2006 measurement campaign on samples from the Kumdykol diamond deposit (sample provided by T. Shumilova). The overlay of rings around the diffraction spots in the pattern in **b** marks the positions of 18 diffraction spots that have been used for lattice parameter refinement with the program UnitCell (Holland and Redfern 1997) to verify the nature of the material by its lattice parameter ($a = 3.577 \pm 0.005$ Å). Note, that the kinematical forbidden diffraction spots (marked with stars) do not appear in the kinematical simulated overlay in Fig. 2b

on Si–C compounds, yielded again only the aforementioned phase, with a nearly perfect lattice match and a FOM value of 4 (Fig. 2d). Contrary to the statement in the report by Shumilova et al. (2011) that the elemental composition of the particles had been verified by energy dispersive X-ray spectroscopy (EDXS), the present author was unable to link one of the few EDX spectra in the TEM archive with these crystals. This prevented post-mortem verification of the suspected chemical composition. Nevertheless, the striking morphologies of this particle, with thickness fringes up to the center region, differs significantly from that of the other constituents found in these samples, particularly all the particles identified as containing carbon only (see Fig. 3 for example). Assuming the validity of the assumption that a

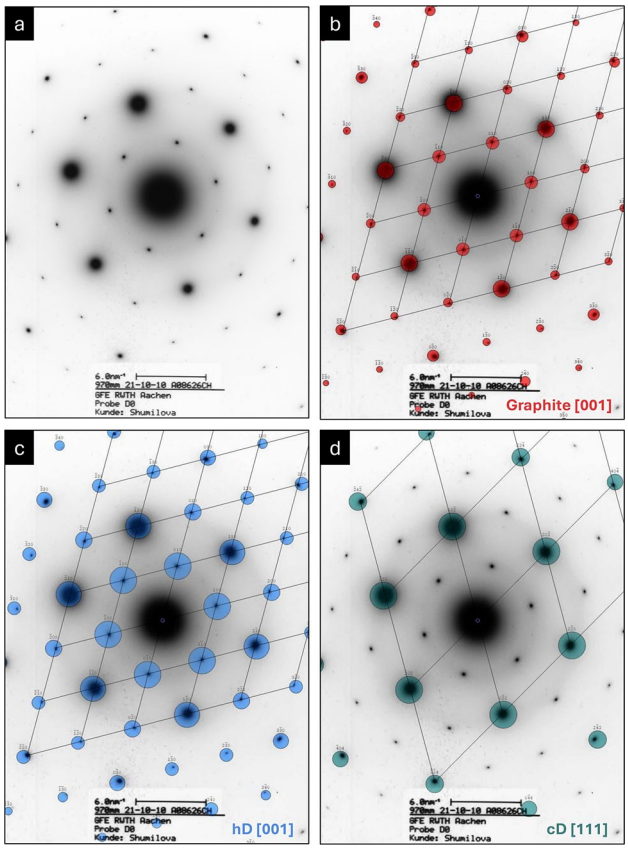

Fig. 4 The SAED pattern in **a**has been originally identified as a two-phase 3C–2H diamond particle by Shumilova et al. (2011). As shown by the simulation of kinematic SAED patterns, this interpretation disregarded the fact that the geometry of the diffraction pattern is also compatible with [001] 2H graphite (PDF# 04-020-4354) in **b**, which matches with all positions of the experimental diffraction spots like 2H diamond (PDF# 04-016-6276) in (**c**). For comparison with **a** the simulated diffraction pattern for 3C diamond (PDF# 01-079-6061) along [111] is shown in **d**, which matches the strong diffraction spots only. This allows interpretation of the pattern in **a** as a topotactic intergrowth of 2H graphite and 3C diamond with the orientation relationship $\{001\}_{2H\,G} \| \{111\}_{3C}$ and $[001]_{2H\,G} \| <111>_{3C}$. Similar intergrowth structures has been observed by Garvie et al. (Garvie et al. 2014) and are known as ´diaphite´ (Németh et al. 2020) (see main text)

HP-SiC is indeed the correct solution, though this remains a highly speculative postulation at present, it is, based on the currently available data, impossible to determine whether this phase is a valid component of the sample and maybe a potential 'signature' for an impact event as proposed in Tretiakova and Lyukhin (2017), or whether it is a contamination. For more on the issues with SiC in recovered samples, readers may refer to Dobrzhinetskaya et al. (2022) who discuss this matter in detail.

Re-assessment for the SAED pattern from an ascribed two-phase 3C-2H diamond particle

Analysis of the second SAED pattern shown in Figs. 1c and 4a with the program *SAED Extension*, revealed that the geometric arrangement of the diffraction spots is compatible with 2H graphite and 2H diamond, thus the earlier approach of using the FOM value to distinguish between different phases proved unreliable. Figure 4b, c illustrate this situation by showing overlays of the simulated SAED patterns for the geometric matches of [001] 2H graphite (PDF# 04-020-4354, $a=2.5714$ Å, $c=6.8382$ Å), [001] 2H diamond (PDF# 04-016-6276, $P6_3/mmc$, $a=2.5239$ Å, $c=4.1213$ Å), and for the strong diffraction spots of [111] 3C diamond (PDF# 01-079-6061, *Fd-3m*, $a=3.577$ Å). It should be noted that the 2H graphite phase with a lattice parameter of $a=2.57$ Å is identical to the phase that was previously identified as a potential solution for the SAED pattern in Fig. 1a. For comparison, regular graphite has a much smaller lattice parameter of approximately 2.46 Å (PDF #00-056-0159) (Howe et al. 2003). To investigate this issue further and determine which phase (2H graphite or 2H diamond) contributed to the diffraction pattern shown in Fig. 4a, additional SAED patterns were used from the same TEM measurement campaign and analysed. This procedure involved first defining and determining the dimensions and angles of the 2D reciprocal unit cell manually and then processing these patterns with the *SAED extension* program. For each SAED pattern, the with *SAED extension* calculated kinematic pattern of the most closely match of 2H graphite and 2H diamond are shown in the supplementary material section (Figures SM-1 to SM-6). A subsequent evaluation of the SAED patterns, with an almost ideal cell angle of 60° in reciprocal space, yielded an average value of 2.536 ± 0.025 Å for the a-axis and $\gamma = 119.9(1)°$ for the 2D projected cell in real space. Two more diffraction patterns (SM-5 and SM-6) with shorter cell axes showed cell angles that significantly deviated from 120° (see Table SM-1). As these are results from data measured with two different TEM´s on the same samples, the larger values observed for the a-axis are considered real. However, to the present author's knowledge, no other study has reported graphite with such large unit cell parameters,

except for the one in the aforementioned high-pressure study (Lei et al. 2013). However, unit cells with nearly this *a*-lattice parameter are reported for 2H diamond and have been proposed by Ownby et al. (1992) for a 4H (PDF# 00-050-1082, $P6_3/mmc$, $a=2.522$ Å, $c=8.237$ Å) and an 8H polytype (PDF# 00-050-1084, $P6_3/mmc$, $a=2.522$ Å, $c=16.474$ Å). The latter 8H polytype, but with a smaller lattice parameter, was later experimentally verified by Wang et al. (Wang et al. 2008) and is a composite structure with 25% 2H and 75% 3C diamond (PDF# 00-061-0282, $P6_3/mmc$, $a=2.479$ Å, $c=16.300$ Å). As the overlay of the calculated pattern intensities for [001] 2H diamond in Fig. 4c does not appear to be compatible with the whole pattern, the simulated patterns for the two calculated polytypes of Ownby et al. appear to match the observed SAED pattern very well geometrically and in terms of their intensity distribution, as demonstrated in Fig. 5b for the 4H polytype structure. This interpretation is in line with Smith et al. (2011), who concluded from an extended analysis of Raman spectra, that Kumdykol diamonds are predominantly composed of mixtures of several sp^3-bonded polytypes (3C, 2*n*H). As illustrated in the supplemental material, all experimental SAED patterns under consideration align within the same category of structures with respect to pattern geometry. However, a distinguishing feature are the varied intensity distributions of the diffracted spots, which in most cases cannot easily be assigned to a single structure or polytype. As demonstrated by the simulated SAED patterns presented in figure SM-7, it is also not restrictive for the interpretation to assume exclusively sp^3 bonded carbon polytypes, since matching patterns can also be obtained with (hypothetical) defect or disordered sp^2 bonded 2H graphite with a lattice parameter similar to that found for the HP-phase PDF# 04-020-4354 ($a=2.5714$ Å, $c=6.8382$ Å). Therefore, it can be postulated that both sp^3 and sp^2 bonded polytypes, in differing proportions, can be utilised to correspond with the experimental SAED patterns. This finding is consistent with the (unproven) claim of Shumilova et al. (2011), who reported the presence of three-phase aggregates of lonsdaleite (2H diamond) monocrystals with cubic 3C diamond and 2H graphite in the samples. However, the latter links with another likely interpretation of the SAED pattern in Figs. 1c and 4a, respectively, which assumes a composite or intergrowth of 2H graphite and 3C diamond with the topotactic orientation relationship $\{001\}_{2H\ G} \parallel \{111\}_{3C}$ and $[001]_{2H\ G} \parallel <111>_{3C}$. Similar intergrowth structures with the same relationship has also been observed by Garvie et al. (2014) in HRTEM images of material from the Gujba meteorite and are known as 'diaphite' (Németh et al. 2020). Furthermore, such 2H graphite–3C diamond intergrowths are also commonly found as inclusions in natural diamonds (Harris 1972; Harris and Vance 1972; Glinnemann et al. 2003) and were recognised by Tretiakova & Lyukhin (2017) as an indicator that the Kumdykol diamond-bearing deposit has been formed as the result of a comet impact that led to the formation of symplectite-like 2H graphite–3C diamond intergrowths and 3C diamond crystals coated with 2H graphite rims. Other researchers (Korsakov et al. 2010) have also suggested that the thick 2H graphite coatings (sometimes larger than 100 µm) found around diamond crystals likely formed during the final stages of ultra-high-pressure (UHP) conditions.

Nevertheless, as can be seen from the above discussion, the interpretation of this type of SAED patterns, and in

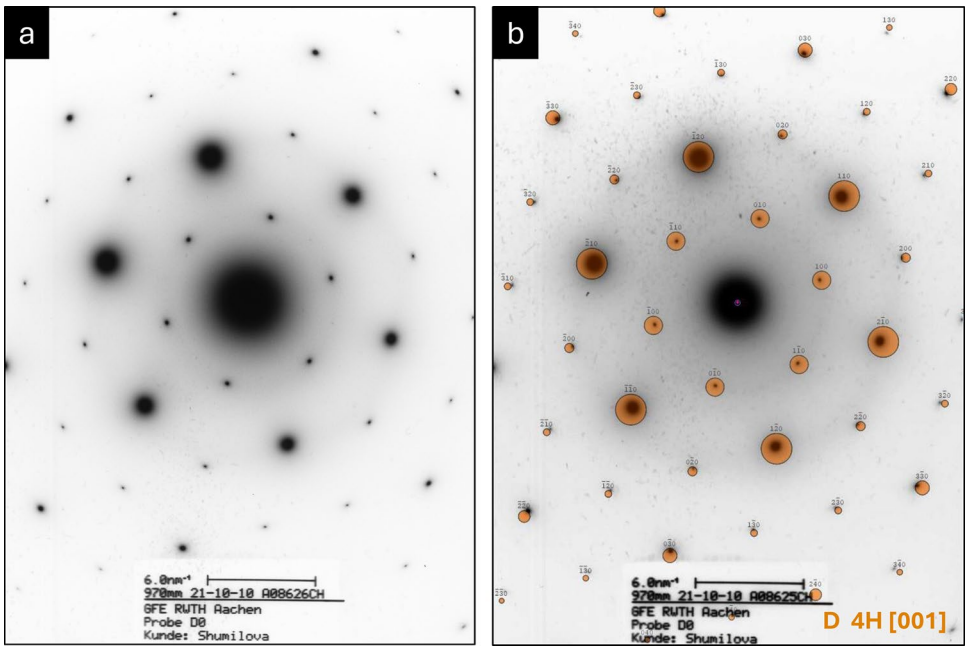

Fig. 5 SAED pattern from Fig. 4 in **a** and pattern of the theoretical proposed hexagonal 4H polytype of carbon (Ownby et al. 1992) in projection along the principal *c*-axis in **b**. It is important to note that the pattern simulation for the 4H polytype (PDF# 00-050-1082, $P6_3/mmc$, $a=2.522$ Å, $c=8.237$ Å) and the 8H polytype (PDF# 00-050-1084, $P6_3/mmc$, $a=2.522$ Å, $c=16.474$ Å) yielded apparently identical results, so only the pattern for the 4H polytype is shown here. As the overlay of the calculated pattern intensities for [001] 2H diamond in Fig. 4c does not appear to be compatible with the whole pattern, the simulated pattern for the 4H polytype matches the observed SAED pattern very well geometrically and in terms of their intensity distribution (see discussion in the main text)

particular the one shown in Figs. 1c and 4a, is not unique, and the currently available experimental data with only one crystallographic projection do not allow a definitive conclusion to be drawn as whether the particle in Fig. 1d is a diaphite made of 2H graphite and 3C diamond (Németh et al. 2020), or if it is an even more complex mixture of polytypes, as suggested by Smith et al. (2011).

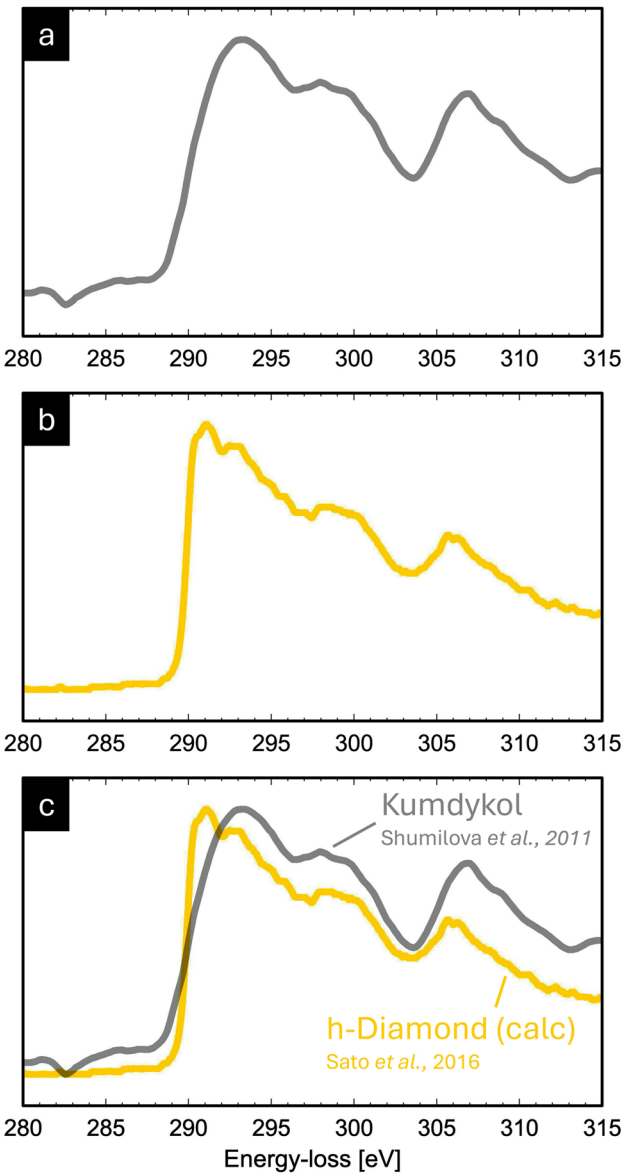

Fig. 6 Extracted EEL spectrum from Shumilova et al. (2011) of a particle in the Kumdykol deposit in **a** and the extracted simulated EEL spectrum for hexagonal 2H diamond from Sato et al. (2016) in **b**. The overlay of both spectra in **c** reveals significant differences in shape between the two. This finding strongly implies that the particle investigated from the Kumdykol deposit is not from a crystal with a 2H diamond structure, as it was claimed by Shumilova et al. (2011)

Re-assessment of the experimental EEL spectrum

In Fig. 2 of their original publication, Shumilova et al. present three carbon K-edge electron energy-loss (EEL) spectra. These include reference spectra for hexagonal 2H graphite and 3C diamond (both taken from the online database eelsdb.eu), as well as one experimental spectrum recorded using the FEI Titan 80–300 STEM transmission electron microscope at the ER-C, Jülich Research Centre (Ernst Ruska-Centre 2016). As with the Raman and EDX spectra shown, the report in Shumilova et al. (2011) contains no additional information, such as TEM images or SAED patterns, that would enable the origin of the presented experimental EEL spectrum to be related to a specific particle. Nevertheless, as the experimental spectrum lacked the prominent π^* peak, which is characteristic for sp^2-bonded carbon, the authors concluded that the spectrum was indicative for the 2H diamond structure.

For the purpose of re-assessment, the EELS data presented in Shumilova et al. (2011) were first reconstructed as XY-pixel values from the enlarged Fig. 2 and then calibrated according to the provided energy-loss scale (see Fig. 6a). To allow comparison with the calculated carbon K-edge EEL spectrum for 2H diamond in Sato et al. (2012); Sato et al. 2016), these data were also reconstructed using Fig. 3 in Sato et al. (2016) (see Fig. 6b). As shown in Fig. 2 in Sato et al. (2016), the calculated EEL spectrum corresponds very well with the measured experimental spectra from 2H diamond (spectrum P1). Thus, the calculated spectrum is considered here as a valid reference for hexagonal 2H diamond. Figure 6c shows a corresponding overlay of the reconstructed EEL spectra for the verified 2H diamond and the data from Shumilova et al. (2011).

As a complementary reference, Fig. 7a shows an EEL spectrum collected by this author in 2006 from a verified 3C diamond crystal, originating from the Kumdykol diamond deposit (the SAED pattern and the corresponding TEM bright-field image are shown in Figs. 3a, c, respectively). Figure 7b shows an overlay of the collected EEL spectrum with the reconstructed spectrum from Shumilova et al. (2011).

A visual comparison of the two overlay images in Figs. 6c and 7c reveals that the match of the experimental EEL spectrum published in Shumilova et al. (2011) is, despite a minimal shift on the energy-loss scale, much better for 3C diamond (sample P19) than with the calculated spectrum for 2H diamond. This finding indicates that the EEL spectrum presented by Shumilova et al. is very likely from 3C diamond and not from 2H diamond. This argument is further strengthened by comparing the calculated EEL spectrum for 2H diamond with a spectrum obtained from

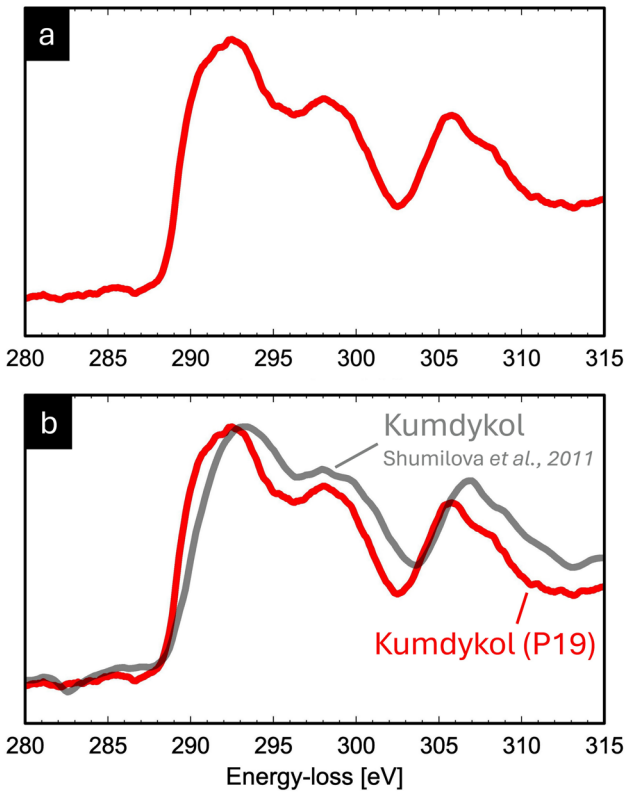

Fig. 7 The EEL spectrum in **a** was recorded from the verified 3C microdiamond shown in Fig. 3, that was found in a sample from the Kumdykol deposit (FEI Tecnai F20 with Gatan GIF2000, acquisition mode: parallel dispersive, illumination mode: TEM, exposure time: 4 s, dispersion: 0.1 eV/channel, Zero-loss FWHM: 0.9 eV, sample name: 'D4', object identifier: 'P19'). Overlaying this with the reconstructed experimental EEL spectrum from Fig. 6a shows the close similarity in intensity of the two spectra. It should be noted, that both spectra show a distinct V-shaped bandgap between the nearly equal height σ* states at approximately 298 eV and 305 eV. This feature is a characteristic fingerprint for the 3C diamond structure and thus indicates that the spectrum from Shumilova et al. (2011) is from 3C diamond and not from 2H diamond. The origin of the visible small energy shift of approximately 1 eV between the two spectra could not be resolved, as the original data used in reference (Shumilova et al. 2011) were unavailable for this reassessment. Reasons for the shift may include spectrum drift during acquisition (which can occur during beam scanning in a STEM), inaccurate calibration of the energy scale, or minor errors introduced during reconstruction from the published figure

material found at the Tunguska impact site (Kvasnytsya et al. 2013). In this case, the close similarity of the two EEL spectra shown in Fig. 8 does indeed allow speculation about the presence of 2H diamond in the sample. A particularly prominent feature common to both spectra is the continuous decrease in intensity following the initial maximum. However, for 3C diamond, a pronounced secondary (V-shaped) bandgap between two σ* states of almost equal intensity at approximately 298 eV and 305 eV exists (see Fig. 7a). This characteristic feature of 3C diamond is also clearly visible in the experimental EEL spectrum shown in Fig. 6a that has

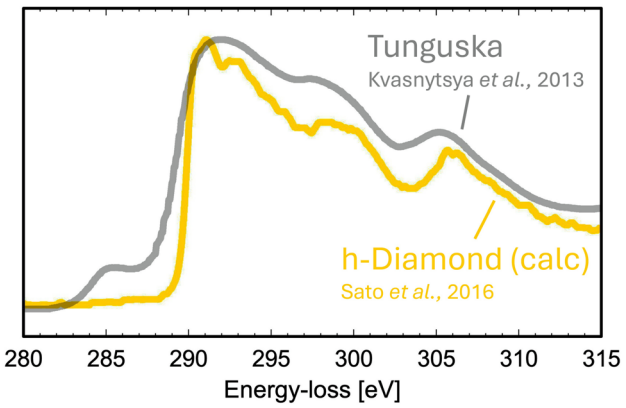

Fig. 8 A comparison of the reconstructed EEL spectrum of a particle described as lonsdaleite from the Tunguska impact site (Kvasnytsya et al. 2013) with the calculated spectrum for hexagonal 2H diamond from Sato et al. (2016) shows a much higher similarity than in Fig. 6c. Notably, the gradual decrease in intensity following the initial peak, accompanied by three sub-maxima, is a common feature. This feature of a continued decrease in intensity is clearly not observable in the experimental EEL spectrum shown in Fig. 6a. Therefore, it is unlikely that the recorded spectrum presented in Shumilova et al. (2011) is related to the 2H diamond structure. The unusual pre-edge EELS feature at around 285 eV in the energy-loss spectrum of the particle recovered from the Tunguska site indicates a diaphite interface, as has also been observed in Murchison nanodiamonds (Németh et al. 2021)

been extracted from Shumilova et al. (2011). After careful consideration of all the relevant details, it can be concluded with a high degree of certainty that the EEL spectrum presented by Shumilova et al. belongs to 3C diamond and not to 2H diamond.

Summary and Conclusion

The re-evaluation of the experimental data used by Shumilova et al. (2011) yielded the following results.

- The geometric and intensity-based re-analysis of an SAED pattern that has been earlier interpreted as monocrystalline 2H diamond reveals that the pattern fits far more convincingly with a high-pressure form of 2H graphite than with any plausible orientation of hexagonal 2H diamond. Even the simulated diffraction pattern for 2H diamond that comes closest to the experimental pattern fails to adequately reproduce the true geometry. Thus, this finding proves the earlier made interpretation as monocrystalline 2H diamond as extremely unlikely. However, it should be noted that the geometry of the SAED pattern in question matches remarkably well with the lattice structure of silicon carbide in its cubic high-pressure form (PDF file #04-006-7620). Moreover, judged from TEM bright field images, this species appears nearly defect-free and is characterised

by thickness fringes extending to the centre of the particles, suggesting an ultrathin sample composed of light elements only. Due to the lack of EDX data for these crystals, it is however not possible in retrospect to determine whether these crystals belong to a carbon phase or to confirm the assumption that they are silicon carbide.

- Another SAED pattern, described as a two-phase 3C diamond–2H diamond particle, exhibits diffraction geometry and a spot intensity modulation that does not allow a unique interpretation. This pattern can be explained by a 2H graphite–3C diamond intergrowth, with the orientation relationship $\{001\}_{2H\ G} \parallel \{111\}_{3C}$ and $[001]_{2H\,G} \parallel <111>_{3C}$. This relationship is consistent with diaphite (Németh et al. 2020), as observed in meteorite remains (Garvie et al. 2014), or with symplectite-like intergrowths and 3C diamonds with 2H graphite rims, recovered from the Kumdy Kol deposit (Korsakov et al. 2010). Furthermore, the experimental pattern is fully compatible with the [001] orientation of proposed sp^3-bonded polytypes 4H and 8H (Ownby et al. 1992; Wang et al. 2008), which is consistent with the findings of an in-depth analysis of the Raman spectra of Kumdy Kol diamonds (Smith et al. 2011).
- The interpretation of an experimental carbon core-loss EEL spectrum shown in Shumilova et al. (2011) falls to short as it was assumed that a missing π^* peak is a unique proof for the presence of 2H diamond. This interpretation ignored, that this argument applies for 3C diamond too, where all carbon atoms are also sp^3 hybridized. Nevertheless, a direct comparison of the experimental spectrum displayed in Shumilova et al. (2011) with the energy-loss near-edge fine structure in a spectrum from a confirmed 3C diamond displays good agreement, whereas the match with a calculated spectrum for the pure 2H form shows only poor similarity.

The re-assessment of the in Shumilova et al. (2011) published SAED and EELS data provide no concrete evidence for the presence of monocrystalline 2H diamond in the earlier examined specimens from the Kumdykol site. It is therefore necessary to correct the aforementioned claims in order to avoid further bias in the ongoing discussion on the nature of the mineral lonsdaleite.

Supplementary Information The online version contains supplementary material available at https://doi.org/10.1007/s00269-025-01331-x.

Acknowledgements The here shown experimental data from cubic micro-diamonds in Fig. 3 were obtained by the present author during an investigation conducted in 2006 on samples provided by Dr. T.G. Shumilova during her research visit at the authors facility. It is the author's best knowledge that these samples originate from the Kumdykol crater in North Kazakhstan, as does the material described in [1].

The author gratefully acknowledges Ms Cleopatra Herwartz and Dr. Dieter Wagner (GFE) for the follow-up investigation in 2010 carried out on another sample from the same site.

Author contributions All presented results of the re-evaluation of the old data were performed by the present author. Credit to Ms C. Herwartz and Dr Dieter Wagner for performing part of the TEM investigations as well as to Dr. Shumilova for providing the materials is given in the acknowledgements.

Funding Open Access funding enabled and organized by Projekt DEAL. No funds, grants, or other support was received.

Data availability The data are currently not public available but can be provided upon request.

Declarations

Conflict of interest The authors declare no competing interests.

References

Bean JJ, Katiyar NK, Forrest RM, Zhou XW, Goel S (2025) Resolving Lonsdaleite's decade-long controversy: atomistic insights into a metastable diamond polymorph. Diamond Relat Mater. https://doi.org/10.1016/j.diamond.2025.112405

Boslough M, Nicoll K, Holliday V, Daulton TL, Meltzer D, Pinter N, Scott AC, Surovell T, Claeys P, Gill J, Paquay F, Marlon J, Bartlein P, Whitlock C, Grayson D, Jull AJT (2012) Arguments and evidence against a Younger Dryas impact event. Clim Landscapes Civilizations 198:13–26. https://doi.org/10.1029/2012GM001209

Chen GW, Zhu SC, Xu L, Li YM, Liu ZP, Hou YL, Mao HK (2024) The transformation mechanism of 2H graphite to hexagonal diamond under shock conditions. JACS 4(9):3413–3420. https://doi.org/10.1021/jacsau.4c00523

Daulton TL, Pinter N, Scott AC (2010) No evidence of nanodiamonds in Younger-Dryas sediments to support an impact event. Proc Natl Acad Sci U S A 107:16043–16047. https://doi.org/10.1073/pnas.1003904107

Daulton TL, Amari S, Scott AC, Hardiman M, Pinter N, Anderson RS (2017) Comprehensive analysis of nanodiamond evidence relating to the Younger Dryas impact hypothesis. J Quat Sci 32(1):7–34. https://doi.org/10.1002/jqs.2892

Dobrzhinetskaya LF, Wirth R, Green HW II (2006) Nanometric inclusions of carbonates in Kokchetav diamonds from Kazakhstan: a new constraint for the depth of metamorphic diamond

crystallization. Earth Planet Sci Lett 243:85–93. https://doi.org/10.1016/j.epsl.2005.11.030
Dobrzhinetskaya LF, O'Bannon EF, Sumino H (2022) Non-cratonic diamonds from UHP metamorphic terranes, ophiolites and volcanic sources. Rev Mineral Geochem 88(1):191–255. https://doi.org/10.2138/rmg.2022.88.04
Ernst Ruska-Centre for Microscopy and Spectroscopy with Electrons (ER-C) (2016) Forschungszentrum Jülich and RWTH Aachen. J Large-Scale Res Facilities 2:A42. https://doi.org/10.17815/jlsrf-2-67
Fan QY, Chai CC, Wei Q, Wong KQ, Liu YQ, Yang YT (2018) Theoretical investigations of group IV alloys in the Lonsdaleite phase. J Mater Sci 53(4):2785–2801. https://doi.org/10.1007/s10853-017-1681-6
Garvie LAJ, Németh P, Buseck PR (2014) Transformation of graphite to diamond via a topotactic mechanism. Am Mineral 99(2–3):531–538. https://doi.org/10.2138/am.2014.4658
Glinnemann J, Kusaka K, Harris J (2003) Oriented 2H graphite single-crystal inclusions in diamond. Zeitschrift Für Kristallographie - Crystalline Mater 218(11):733–739. https://doi.org/10.1524/zkri.218.11.733.20302
Greshnyakov VA, Belenkov EA (2017) Investigation on the formation of lonsdaleite from 2H graphite. J Exp Theor Phys 124:265–274. https://doi.org/10.1134/S1063776117010125
Harris JW (1972) Black material on mineral inclusions and in internal fracture planes in diamond. Contr Mineral Petrol 35:22–33. https://doi.org/10.1007/BF00397374
Harris JW, Vance ER (1972) Induced graphitisation around crystalline inclusions in diamond. Contr Mineral Petrol 35:227–234. https://doi.org/10.1007/BF00371217
Holland TJB, Redfern SAT (1997) J. UNITCELL: a nonlinear least-squares program for cell-parameter refinement and implementing regression and deletion diagnostics. J Appl Crystallogr 30(1):84. https://doi.org/10.1107/S0021889896011673
Howe J, Rawn C, Jones L, Ow H (2003) Improved crystallographic data for graphite. Powder Diffr 18:159. https://doi.org/10.1154/1.1556991
Jones AP, McMillan PF, Salzmann CG, Alvaro M, Nestola F, Prencipe M, Dobson D, Hazael R, Moore M (2016) Structural characterization of natural diamond shocked to 60 GPa; implications for Earth and planetary systems. Lithos 265:214–221. https://doi.org/10.1016/j.lithos.2016.09.023
Kabekkodu SN (2024) PDF-5+: a comprehensive Powder Diffraction File™ for materials characterization. Powder Diffract 39(2):47–59. https://doi.org/10.1017/S0885715624000150
Korsakov AV, Perraki M, Zedgenizov DA, Bindi L, Vandenabeele P, Suzuki A, Kagi H (2010) Diamond–2H graphite relationships in Ultrahigh-pressure metamorphic rocks from the Kokchetav Massif, Northern Kazakhstan. J Petrol 51(3):763–783. https://doi.org/10.1093/petrology/egq001
Kvasnytsya V, Wirth R, Dobrzhinetskaya L, Matzel J, Jacobsen B, Ian Hutcheon I, Tappero R, Kovalyukh M (2013) New evidence of meteoritic origin of the Tunguska cosmic body. Planet Space Sci 84:131–140. https://doi.org/10.1016/j.pss.2013.05.003
Lei L, Yin W, Jiang X, Lin S, He D (2013) Synthetic route to metal nitrides: high-pressure solid-state metathesis reaction. Inorg Chem 52(23):13356–13362. https://doi.org/10.1021/ic4014834
McLaren AC (1991) Transmission electron microscopy of minerals and rocks, 2nd edn. Cambridge University Press, Cambridge
Murri M, Smith RL, McColl K, Hart M, Alvaro M, Jones AP, Németh P, Salzmann CG, Corà F, Domeneghetti MC, Nestola F, Sobolevv N, Vishnevsky SA, Logyinova AM, McMillan PF (2019) Quantifying hexagonal stacking in diamond. Sci Rep 9:10334. https://doi.org/10.1038/s41598-019-46556-3
Németh P, Garvie L, Aoki T et al (2014) Lonsdaleite is faulted and twinned cubic diamond and does not exist as a discrete material. Nat Commun 5:5447. https://doi.org/10.1038/ncomms6447
Németh P, McColl K, Smith RL, Murri M, Garvie LAJ, Alvaro M, Pécz B, Jones AP, Corà F, Salzmann CG, McMillan PF (2020) Diamond-graphene composite nanostructures. Nano Lett 20(5):3611–3619. https://doi.org/10.1021/acs.nanolett.0c00556
Németh P, McColl K, Garvie LAJ, Salzmann CG, Pickard CJ, Corà F, Smith RL, Mezouar M, Howard CA, McMillan PF (2021) Diaphite-structured nanodiamonds with six- and twelve-fold symmetries. Diamond Relat Mater 119:108573. https://doi.org/10.1016/j.diamond.2021.108573
Németh P, Lancaster HJ, Salzmann CG, McColl K, Fogarassy Z, Garvie LAJ, Illés L, Pécz B, Murri M, Corà F, Smith RL, Mezouar M, Howard CA, McMillan PF (2022) Shock-formed carbon materials with intergrown sp3- and sp2-bonded nanostructured units. Proc Natl Acad Sci U S A 119(30):e2203672119. https://doi.org/10.1073/pnas.2203672119
Németh P, Garvie LAJ, Salzmann CG (2023) Canyon Diablo lonsdaleite is a nanocomposite containing c/h stacking disordered diamond and diaphite. Philos Trans R Soc Lond A Math Phys Eng Sci 381(2259):20220344. https://doi.org/10.1098/rsta.2022.0344
Ownby PD, Yang X, Liu J (1992) Calculated X-ray diffraction data for diamond polytypes. J Am Ceram Soc 75:1876–1883. https://doi.org/10.1111/j.1151-2916.1992.tb07211.x
Sato Y, Terauchi M, Inami W, Yoshiasa A (2012) High energy-resolution electron energy-loss spectroscopy analysis of dielectric property and electronic structure of hexagonal diamond. Diamond Relat Mater 25:40–44. https://doi.org/10.1016/j.diamond.2012.02.013
Sato Y, Bugnet M, Terauchi M, Botton GA, Yoshiasa A (2016) Heterogeneous diamond phases in compressed 2H graphite studied by electron energy-loss spectroscopy. Diamond Relat Mater 64:190–196. https://doi.org/10.1016/j.diamond.2016.02.010
Shumilova TG, Mayer E, Isaenko SI (2011) Natural monocrystalline lonsdaleite. Dokl Earth Sci 441(1):1552–1554. https://doi.org/10.1134/S1028334X11110201
Smith DC, Dobrzhinetskaya LF, Godard G, Green HW (2011) Diamond–lonsdaleite–graphite relations examined by raman mapping of carbon microinclusions inside zircon at Kumdy Kol, Kokchetav, Kazakhstan: evidence of the Metamictization of diamond. In: Dobrzhinetskaya LF, Faryad SW, Wallis S, Cuthbert S (eds) Ultrahigh-pressure metamorphism: 25 years after the discovery of coesite and diamond. Elsevier, Amsterdam, pp 43–75
Thomas R, Davidson P, Rericha A, Recknagel U (2023) Ultrahigh-pressure mineral inclusions in a crustal granite: evidence for a novel transcrustal transport mechanism. GEOSCIENCES 13(4):94. https://doi.org/10.3390/geosciences13040094
Tomkins AG, Wilson NC, MacRae C, Salek A, Field MR, Brand HEA, Langendam AD, Stephen NR, Torpy A, Pintér Z, Jennings LA, McCulloch DG (2022) Sequential lonsdaleite to diamond formation in ureilite meteorites via in situ chemical fluid/vapor deposition. Proc Natl Acad Sci U S A 119(38):e2208814119. https://doi.org/10.1073/pnas.2208814119
Tretiakova L, Lyukhin A (2017) Impact–cosmic–metasomatic origin of microdiamonds from Kumdy-Kol deposit, Kokchetav Massiv, N. Kazakhstan. Int Kimberlite Conf. https://doi.org/10.29173/ikc3876
Turneaure SJ, Sharma SM, Volz TJ, Winey JM, Gupta YM (2017) Transformation of shock-compressed graphite to hexagonal diamond in nanoseconds. Sci Adv 3(10):eaao3561. https://doi.org/10.1126/sciadv.aao3561
Wang Z, Zhao Y, Zha C-S, Xue Q, Downs RT, Duan R-G, Caracas R, Liao X (2008) X-ray induced synthesis of 8H diamond. Adv Mater 20:3303–3307. https://doi.org/10.1002/adma.200800052

Weirich TE (2025) UnitCellSAED—an ImageJ-based tool for determining unit cell parameters from selected area electron diffraction patterns. RWTH publications. https://doi.org/10.18154/RWTH-2025-04291

Yoshida M, Onodera A, Ueno M, Takemura K, Shimomura O (1993) Pressure-induced phase transition in SiC. Phys Rev B 48:10587. https://doi.org/10.1103/PhysRevB.48.10587

Zhu SC, Chen GW, Yuan XH, Cheng Y, Wan MH, Xu BY, Wang MS, Tang H, Hou YL (2025) Key for hexagonal diamond formation: theoretical and experimental study. J Am Chem Soc 147(2):2158–2167. https://doi.org/10.1021/jacs.4c16312